Journal of Nuclear Materials 398 (2010) 122–128

Contents lists available at ScienceDirect

Journal of Nuclear Materials

journal homepage: www.elsevier.com/locate/jnucmat

Investigation of the effect of lead–bismuth eutectic on the fracture properties of T91 and 316L

G. Coen [a,b,*], J. Van den Bosch [a,b], A. Almazouzi [a], J. Degrieck [b]

[a] SCK·CEN (Belgian Nuclear Research Centre), Boeretang 200, B-2400 Mol, Belgium
[b] Materials Science and Engineering, Ghent University, Technologiepark 903, B-9052 Zwijnaarde (Ghent), Belgium

A B S T R A C T

Liquid metal embrittlement (LME) may decrease the mechanical integrity of the structure. Therefore quantification of the embrittlement effects by fracture mechanics assessment is highly needed for possible future licensing. Conventional fracture mechanics methods however cannot be applied to tests in liquid metal environment due to the opaque and conducting nature of lead–bismuth eutectic (LBE). Therefore new methods for assessment of plane strain fracture toughness in LBE were examined. The plane strain fracture toughness of T91 and 316L in liquid lead–bismuth environment at 200 and 300 °C is compared with the results obtained in air. The fracture toughness of T91 decreases in LBE while sufficient ductility remains, whereas the toughness of 316L is less affected.

1. Introduction

Future accelerator driven systems (ADS) could provide one of the solutions for the nuclear waste problem by enabling transmutation of minor actinides and long lived fission products. An example of an ADS system currently under development is the MYRRHA project at SCK·CEN.

For MYRRHA as well as for other experimental spallation sources such as MEGAPIE and J-PARC, lead–bismuth eutectic (LBE) was chosen as a coolant and/or spallation neutron source [1–3]. For these applications, the European reference candidate structural materials are the ferritic–martensitic steel T91 for the parts working at high temperatures under high neutron doses and the austenitic stainless steel 316L for the parts working at lower operating temperature and lower neutron flux components.

The compatibility of the structural materials with the liquid lead–bismuth is known to be one of the critical issues in the development of the ADS. Therefore liquid metal embrittlement (LME) needs to be examined carefully since it may cause premature brittle fracture of an otherwise ductile material when the material is placed in direct contact with the liquid metal under stress. Moreover various parameters such as not only strain rate and temperature [4] but also stress concentrators, hardness, composition, etc. are known to influence the susceptibility of the considered steels to LME [5–8].

Most of the knowledge on this topic was established by performing tensile tests [9]. Results on the susceptibility of 316L steel to LME are much scarcer than on T91 steel because it is generally accepted that the effect of the LBE on the mechanical properties (e.g. the low-cycle fatigue behaviour [10]) of the former is very limited. To enable the future construction of the ADS, it is however needed to quantify the embrittlement by means of fracture toughness tests in LBE. A very limited amount of fracture toughness data is currently available due to difficulties involved with testing because the opaque and conducting nature of LBE makes it impossible to use the conventional test and analysis methods such as described in ASTM E-1820. As a result, different authors have used different experimental methods in an attempt to solve this problem. For instance, Long and Dai [11] examined LME by performing 3-point bending tests in an LBE environment to assess the plane strain fracture toughness of T91 ferritic–martensitic steel at 200, 300, 400 and 500 °C. The fracture toughness values were obtained by using a correlation between crack length and actuator displacement, determined using multispecimen technique. Results showed a reduction of the J-values of 20–30% in presence of LBE for non-hardened T91 at 200 °C. Auger et al. [12] used centre cracked in tension specimens (CCT) to try to assess the plane stress fracture toughness of T91 steel. Crack growth was monitored optically by using a very limited amount of LBE. It was concluded that the embrittlement of T91 steel by LBE is significantly low, so, according to Auger et al. [12], LME of non-irradiated T91 by LBE is not a relevant concern for design.

In [13], normalisation methods (normalisation data reduction NDR (ASTM E-1820) and the single specimen methods described by Donoso et al. [14] and by Chaouadi [15]) were used to

* Corresponding author. Address: SCK·CEN (Belgian Nuclear Research Centre), Boeretang 200, B-2400 Mol, Belgium. Tel.: +32 14 333178; fax: +32 14 321216.
E-mail address: Gunter.Coen@sckcen.be (G. Coen).

0022-3115/$ - see front matter © 2009 Elsevier B.V. All rights reserved.
doi:10.1016/j.jnucmat.2009.10.021

determine the plane strain fracture toughness values of T91 at 200 °C in a stagnant LBE environment. These normalisation methods were originally developed to enable the analysis of fracture toughness tests in the ductile, upper shelf regime in aggressive environments where conventional methods can not or can hardly be applied. In these methods, only the force–displacement data and the initial and final crack length are used as inputs for fracture toughness determination.

This paper discusses the effect of LBE on the plane strain fracture toughness of ferritic–martensitic T91 steel and austenitic stainless 316L steel at 200 °C and 300 °C for tests performed at a displacement rate of 0.25 mm $(\text{min})^{-1}$. The fracture toughness is determined using three different normalisation methods described in an earlier paper [13].

2. Experimental

The austenitic stainless steel 316L and the ferritic–martensitic steel T91 were both delivered as hot rolled and heat treated plates with a thickness of 15 mm by Industeel, ArcelorMittal group. The 316L plate was solution annealed at 1050–1100 °C, followed by a water quench. The heat treatment of the T91 plate consisted of a normalisation treatment at 1100 °C for 15 min followed by a water quench to room temperature. This plate was then tempered by heating the normalized steel to 770 °C for 45 min followed by air cooling to room temperature. The chemical compositions both steels are given in Table 1.

The lead–bismuth eutectic (LBE) was delivered by Hetzel Metalle GmbH, Germany and contains 44.8 wt.% Pb, 55.2 wt.% Bi, 2 mg/g Cr and less then 1 mg/g Ni.

Disc shaped compact tension specimens (DCT, Fig. 1) were machined so the crack plane is situated in the centre of the thickness of the plate and then precracked in fatigue to a crack length of $a = 1/2W = 5$ mm, where a is the crack length and W is the width of the specimen (Fig. 1). After precracking, the specimens were side-grooved at each side to a depth of 10% of the specimen's thickness. These side grooves are needed to limit or prevent a plane stress state at the specimen side surface which would result in shear lips [16] and in an increase in fracture toughness due to an increase in the plastic zone size [17].

Fracture toughness tests were performed on DCT specimens of both T91 and 316L steels, in air and in oxygen saturated LBE environments. All tests discussed in this paper were performed at a displacement rate of 0.25 mm $(\text{min})^{-1}$. Test temperatures were 200 and 300 °C.

The tests in air are considered to be reference tests to quantify the fracture toughness (J–R curve, which is a plot of the crack extension resistance as a function of the crack extension for elastic nonlinear materials, and the value of the J-integral at initiation of crack extension, J_Q) of the materials using the specimen shape described above. Different single specimen techniques were used to monitor the crack growth during the tests in air, namely unloading compliance (UC) and potential drop (PD). The former uses the compliance of the specimen measured during periodic unloadings by means of a clip gauge extensometer for accurate measurement, while the latter measures the potential difference across the specimen to determine the size of the advancing crack. Unfortunately, both techniques are not applicable in LBE environment. This is due to the fact that at one hand the conducting nature of the LBE penetrating the crack hinders the measurement of the potential difference over the crack and on the other hand the compliance cannot be measured accurately since the clip gauge extensometer will be chemically attacked by LBE. Therefore, only the force–displacement data, consisting of the deformation of the load line and the crack mouth opening displacement (CMOD), which is the crack displacement due to elastic and plastic deformation measured by the clip gauge extensometer at the mouth of the crack (Fig. 1), were available for tests in LBE.

Alternatively, normalisation methods, such as the normalisation data reduction method (NDR, ASTM E-1820) and the single specimen methods described by Donoso et al. [14] and by Chaouadi [15], could be applied to analyze the test data recorded during tests in LBE environment. By using a single specimen method, a full J–R curve can be determined from one single test. The main advantage of the normalisation methods is the fact that they use only the force–CMOD data (recorded by a clip gauge) and the initial and final crack length to calculate the J–R curves of the test. The initial and final crack sizes were determined from the post mortem fracture. The force–CMOD was not readily available for tests in LBE environment because a clip gauge could not be used in this environment, so only force–displacement data were available. The use of force–displacement data instead of force–CMOD data as input for the normalisation methods would however limit their accuracy, since CMOD data consists only of the opening at the crack mouth of the specimen, whereas displacement data consists of both the CMOD and of the deformation of the load line. The measured displacement was therefore corrected using a linear fit of

Table 1
Chemical composition of ferritic–martensitic T91 and austenitic 316L (wt.%).

	C	N	Al	Si	P	S	Ti	V	Cr	Mn	Ni	Cu	As	Nb	Mo	Sn	W
316L	0.02	0.0293	0.018	0.67	0.032	0.0035	0.006	0.07	16.73	1.81	9.97	0.23		0.00	2.05		0.02
T91	0.10	0.0442	0.015	0.22	0.021	0.0004	0.003	0.21	8.99	0.38	0.11	0.06	0.008	0.06	0.89	0.004	0.01

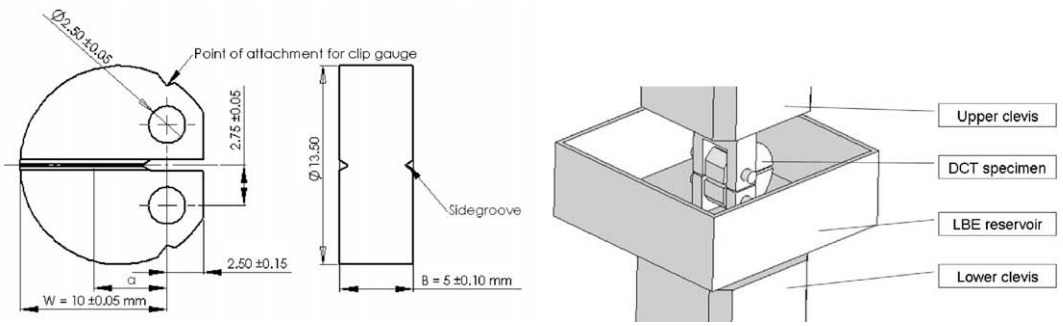

Fig. 1. Schematic representation of: (left) the disc shaped compact tension specimen, dimensions in mm; (right) the test setup used during these experiments.

the force as function of the (displacement–CMOD) obtained from the tests in air, where both clip gauge and displacement data were available. In this way, an approximation of the CMOD data was calculated. An example and the verification of this compliance correction can be found in [13]. All the necessary input for the normalisation methods was thus available for the analysis of tests performed in both environments.

The tests in LBE were performed in the oven of a tensile testing machine. The oven was heated up to about 200 °C and the liquid LBE was then poured into the reservoir, attached to the load line (Fig. 1), until the specimen was submersed. The submersed specimen was then heated up to the test temperature, which was measured by a thermocouple placed in the liquid metal reservoir. After reaching the test temperature, the experiment was held at constant temperature for 20 min to ensure a homogeneous temperature of the specimen and the LBE before starting the test. The test was stopped after an estimated crack growth of about 1 mm. Although there was no online crack measurement, the crack size was estimated using the force–displacement curve. After testing, a solution of hydrogen peroxide, acetic acid and ethanol in a ratio of 1/1/1 was used to remove the LBE of the specimen.

The tests in air were performed using the same load line but without the reservoir. The removal of the reservoir however had no effect on the compliance of the load line of the tensile testing machine. For these tests, the thermocouple was placed in direct contact with the specimen.

The dimensions of the DCT specimens used in these experiments are smaller than recommended by the ASTM E-1820 standard, but were necessary to allow comparison with planned fracture toughness tests on irradiated specimens. By comparing test results of the same type and size specimens in different environment, the effect of LBE on the fracture toughness can be estimated quantitatively.

Before analyzing the results of tests in LBE environment, the feasibility of using the three normalisation methods was verified for our application. The different methods were applied to the force–CMOD test data recorded by the clip gauge used during tests in air. These results were then compared with the results of the unloading compliance and potential drop techniques. In [13], it was shown that the proposed normalisation methods are in good agreement with the conventionally used methods based on online crack advancement monitoring.

One of the problems of performing tests in LBE environment is the reproducibility of the test results. Not all of the specimens were embrittled by the LBE and the specimens that did show signs of embrittlement were not all embrittled to the same extent, presumably due to wetting problems or due to the presence of air bubbles in the precrack. The results thus showed a rather large scatter. As well known, one of the prerequisites of LME is the intimate contact between the steel and the liquid metal, which can be inhibited by air bubbles in the precrack and by the native oxide layer of the steel. When wetting of the steel by LBE does occur, there are clear signs of embrittlement as can be seen in the test results presented in this paper. The presence of air bubbles in the precrack could be prevented in future tests by testing in a closed autoclave where the liquid metal is introduced after evacuating the atmospheric gasses.

In this paper, we have chosen to compare the average J–R curve and J_Q value of the tests performed in air with those of the test in LBE that showed the highest amount of embrittlement. In that way the upper limit of the effect of LME on the fracture toughness properties of the two steels was studied.

3. Results and discussion

3.1. T91 ferritic–martensitic steel

T91 steel was tested at both 200 and 300 °C, in air and oxygen saturated LBE environment at a displacement rate of 0.25 mm (min)$^{-1}$. Fig. 2A shows the results of fracture toughness tests at 200 °C in air and in LBE. The J–R curve was constructed and the J_Q value was calculated for each of the tests in air by using the unloading compliance and potential drop techniques and by applying the different normalisation methods. The average J_Q value is 223 kJ m^{-2} and the average J–R curve of the tests in air at 200 °C is shown in Fig. 3A together with the expected ±15% scatter range.

According to [18], there is a direct correlation between the fracture mechanism and the shape of the recorded load–displacement curves. Thus, from the shape of the curve of the test in air (Fig. 2A), a ductile fracture mechanism could be expected. This was confirmed by the SEM picture of the fracture surface shown in Fig. 4A. On the left, an overview of the fracture surface is shown, the dashed box marks the surface created during the test. A detail of the surface, given on the right, shows that the specimen fractured due to a ductile fracture mechanism (void nucleation, growth and coalescence) resulting in the dimpled fracture surface, which was observed in almost all of the specimens tested in these conditions.

The force data T1 and T2, tested in LBE at 200 °C (Fig. 2A), decreased much faster than the other curves, which is a sign of embrittlement. These two tests exhibited the largest amount of embrittlement according to their force–displacement curves. The J–R curves and J_Q values were calculated for each test (LBE, 200 °C) by applying the three normalisation methods to the force–displacement data from which the compliance was corrected. The J_Q value of specimen T1 (average of the three methods) is 174 kJ m^{-2}, a difference of about 30% with the average value of the tests in air. The average J–R curve of specimen T1 is shown in Fig. 3A together with the ±15% scatter range. This curve is considerably lower than the average curve in air, which also indicates embrittlement.

SEM pictures of the fracture surface were examined so the embrittlement of specimen T1 could be confirmed (Fig. 4B). The

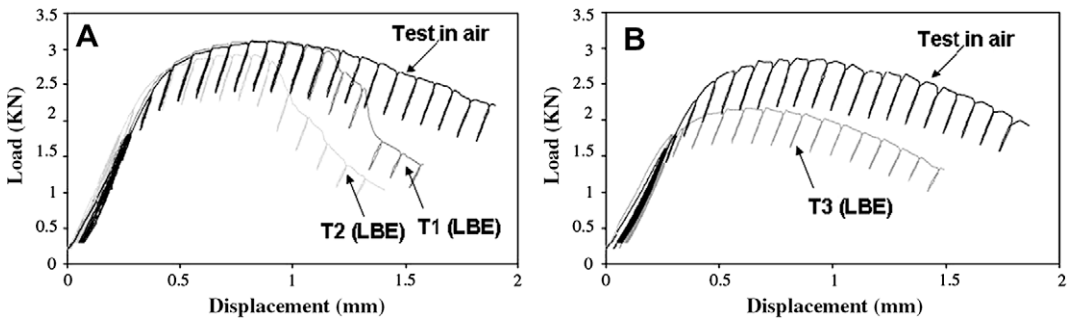

Fig. 2. Force–displacement curves of tests on T91 ferritic–martensitic steel. (A) Performed at 200 °C and 0.25 mm (min)$^{-1}$. (B) Performed at 300 °C and 0.25 mm (min)$^{-1}$.

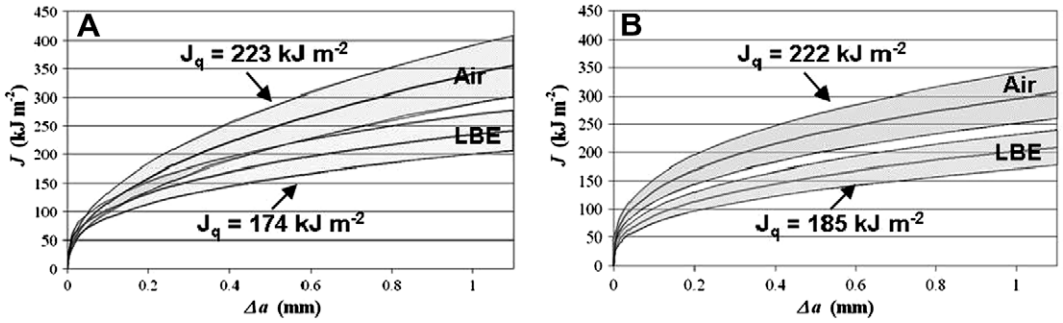

Fig. 3. *J–R* curves of T91 steel tested in air and in oxygen saturated LBE. The *J*-integral value at initiation (J_Q) and the ±15% scatter range are indicated. (A) For tests at 200°. (B) For tests at 300 °C.

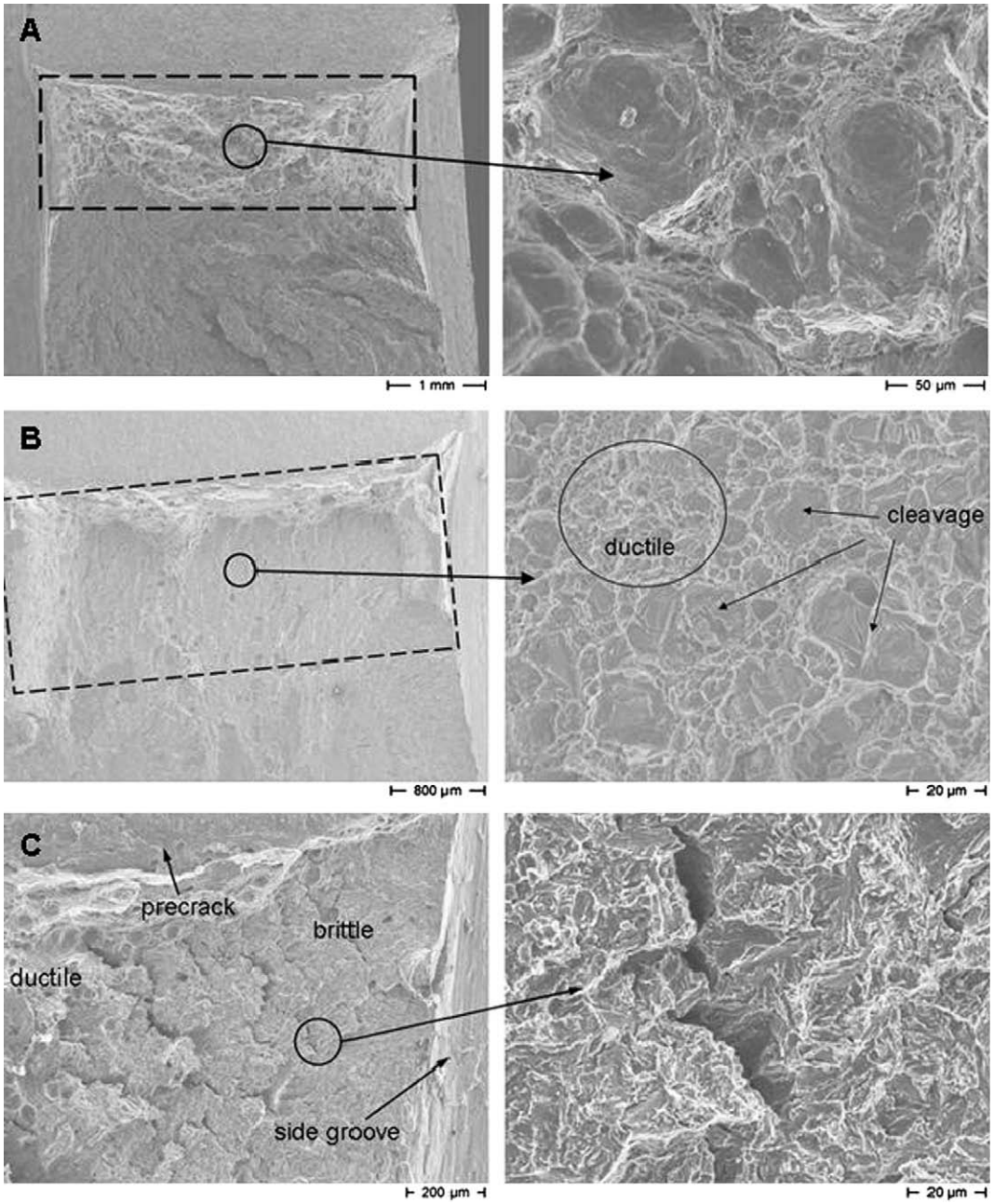

Fig. 4. Fracture surfaces of T91 steel, the dashed box marks the crack measured during the test. (A) Specimen tested at 200 °C in air. The right picture shows the dimpled ductile fracture surface. (B) Test in oxygen saturated LBE environment at 200 °C. The right picture shows a detail of the mixed ductile and brittle fracture surface. (C) Specimen tested in LBE at 300 °C, ductile fracture in the middle of the specimen and more brittle fracture on the side of the specimen, with a magnification of the mixed brittle-ductile fracture surface on the right picture.

left picture shows an overview of the surface fractured during the test. The right picture depicts a detail of the fracture surface. It clearly shows a mixed ductile–brittle fracture surface. In Fig. 4B, several grains which were cracked in cleavage mode indicated by arrows. A region with relatively high fraction of dimples is circled. The embrittlement in the force–displacement and average *J*–*R* curve was thus confirmed by the appearance of the fracture surface of the specimen. Specimen T1 was the most embrittled specimen in our tests and thus serves here as a worst case for LME of T91 at 200 °C.

As an example, Fig. 2B shows the force–displacement curves of tests performed in air and LBE at 300 °C. The average J_Q value of the tests in air is 222 kJ m^{-2} and the average *J*–*R* curve is depicted in Fig. 3B. The test data and fracture toughness value point out the ductile nature of the material which is confirmed by the dimpled fracture surface observed on the SEM pictures.

For tests in LBE environment at 300 °C, there were no force–displacement curves that exhibited the large decrease in force data as observed at 200 °C. However, it seems that there are other signs of embrittlement at 300 °C. Although the number of tests is relatively small and the statistical scatter is rather large, it seems that the maximum of the force–displacement curve of specimen T3 (Fig. 2B) is significantly lower compared to the maximum force of the tests in air due to the effect of the LBE environment.

The *J*–*R* curve of specimen T3 (average of three normalisation methods) is situated lower than the average *J*–*R* curve of the tests in air (Fig. 3B). The difference between the curves is larger than the scatter on both curves, possibly indicating embrittlement. This possible embrittlement is also pointed out by comparing the J_Q values: 222 kJ m^{-2} as average for the test in air at 300 °C and 185 kJ m^{-2} for specimen T3 tested in LBE at the same temperature.

The SEM pictures of the fracture surface of specimen T3 (Fig. 4C) confirmed the embrittlement. The left picture shows the precrack and side groove. The more brittle fracture on the side of the DCT specimen was initiated in the side groove. In the middle of the specimen there is a ductile area, probably due to inadequate penetration of LBE in the crack near the middle of the specimen. The right picture shows a magnification of the mixed brittle-ductile fracture surface. The embrittlement of specimen T3 by LBE is thus visible in the force–displacement data, in the J_Q values, in the *J*–*R* curves and in the SEM pictures of the fracture surface, but although there is embrittlement of the T91 steel by the LBE, there is still sufficient ductility left to prevent brittle failure.

3.2. Austenitic stainless steel 316L

DCT specimens of austenitic stainless steel 316L were tested at 200 and 300 °C in both air and oxygen saturated LBE environment. As for the T91 steel, the tests in air were analyzed by using unloading compliance and potential drop techniques and by applying the three different normalisation methods (NDR, and the single specimen methods described by Donoso et al. [14] and by Chaouadi [15]). For the tests in LBE environment, the force–displacement data were recorded and then analyzed using the three normalisation methods.

Fig. 5A illustrates force–displacement curves of 316L specimens tested in air and in LBE environment at 200 °C. The curves recorded during the tests in air all indicate a ductile behaviour of the 316L steel.

After the tests, the *J*-integral at initiation (J_Q value) was calculated using the $J - \Delta a$ data. The average J_Q value of the 316L steel in air at 200 °C was 258 kJ m^{-2}.

SEM pictures of the fracture surfaces of these tests (Fig. 6A) show the expected dimpled fracture surface. The left picture shows an overview of the fracture surface, the crack measured during the test is indicated by the dashed box on the picture. The flat parts of the fracture surface are a result of deformations caused by breaking of the specimen after the test and were thus not created during the test. The right picture shows a detail of the ductile fracture surface, confirming that the specimen cracked in a ductile manner.

There were almost no clear signs of LME noticeable when comparing the test data of tests at 200 °C in LBE and in air. Only the curve depicted in Fig. 5A shows a slight decrease in force which may be a sign of embrittlement.

The *J*–*R* curves and the J_Q values were calculated for each test. The lowest average J_Q value calculated was 232 kJ m^{-2}, a difference of about 10% with the average value in air (258 kJ m^{-2}). This 10% difference is within the expected scatter range, so it is not a clear sign of embrittlement.

The SEM pictures of the fracture surface of tests performed in LBE environment (Fig. 6B) showed a fully dimpled fracture surface, which was similar to that of the tests performed in air. Therefore, it is concluded that the LBE did not cause any visible change in fracture mechanism of 316L steel. At 200 °C there were thus no obvious signs of LME of 316L steel by LBE.

Fig. 5B shows the test results of fracture toughness tests of 316L performed at 300 °C in air and in LBE environment. The average J_Q value for all of the tests in air at 300 °C was 199 kJ m^{-2}. The SEM picture of the fracture surface shows a fully ductile fracture surface, which is very similar to that of tests at 200 °C (Fig. 6A). These SEM pictures confirm the ductility observed in the force–CMOD curves and in the J_Q value.

Although most of the recorded curves are quite smooth and show no clear signs of LME, the force displacement curve depicted in Fig. 5B, which was obtained at 300 °C in LBE environment, showed some small drops in force.

The J_Q value was calculated to see if the small drops in force were also visible in the fracture toughness results. An average value was calculated for each test. The lowest average value for tests

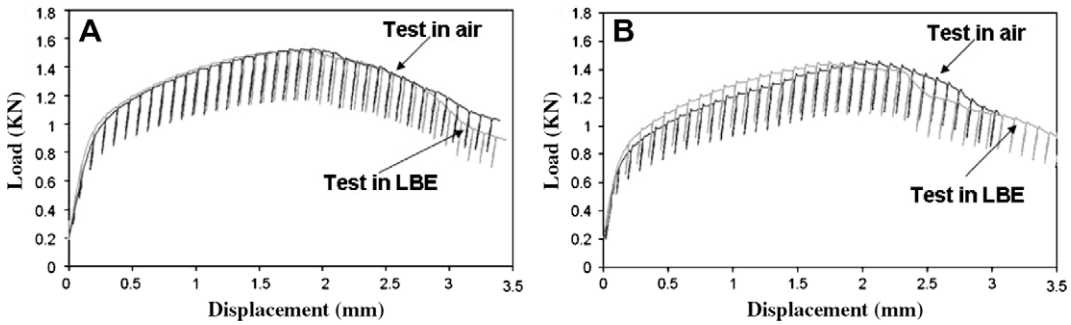

Fig. 5. Force–displacement curves of tests on austenitic stainless steel 316L in air and in oxygen saturated LBE at 0.25 mm (min)$^{-1}$. (A) Tests performed at 200 °C. (B) Tests performed at 300 °C.

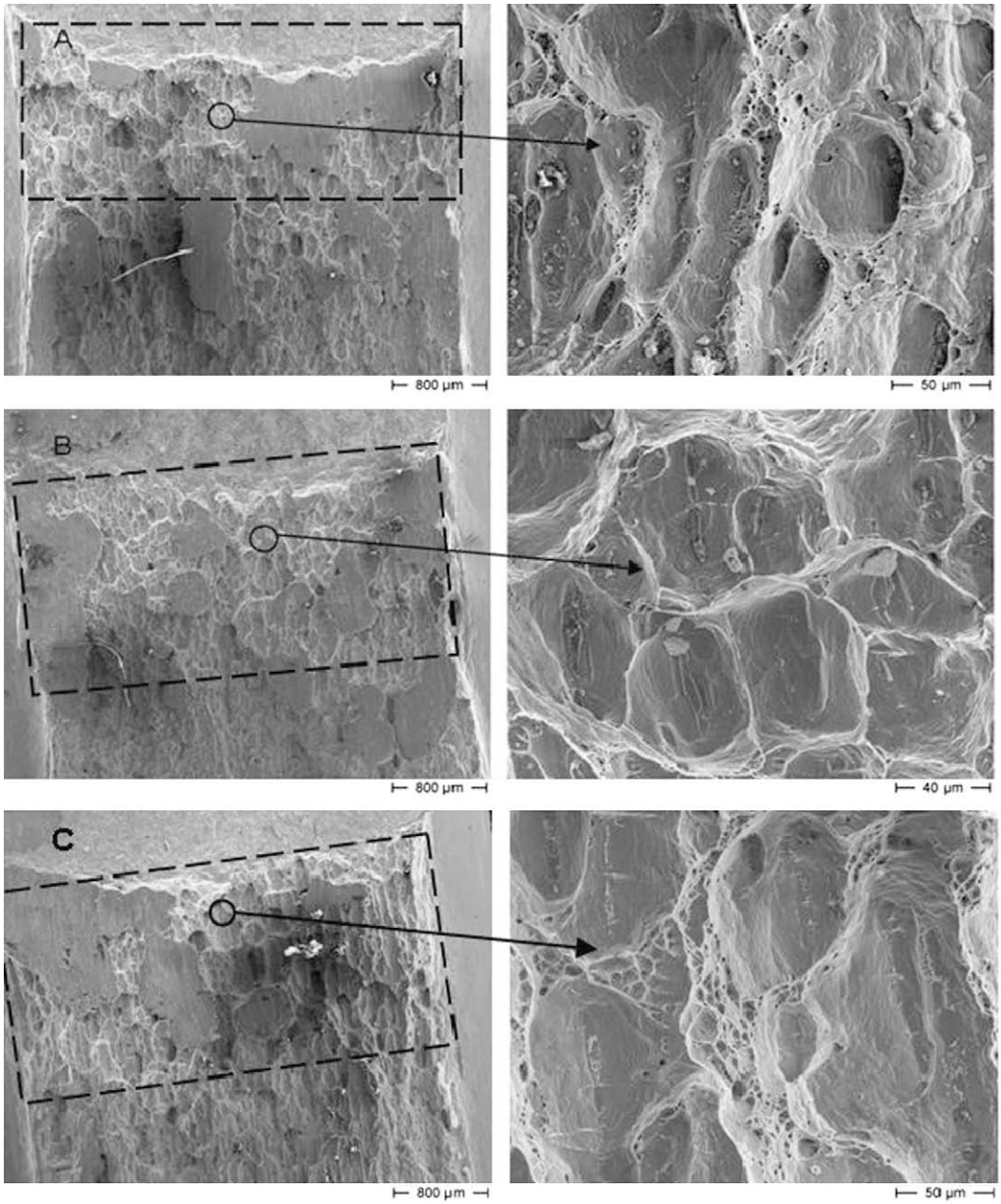

Fig. 6. Fracture surfaces of 316L steel, the flat areas are a result of breaking the specimen after testing. (A) Ductile fracture surface of specimen tested at 200 °C in air. (B) Test in oxygen saturated LBE environment at 200 °C. The right picture shows a detail the ductile fracture surface. (C) Fracture surface of specimen tested in LBE at 300 °C, the magnification of the fracture surface shows no effect of LME by LBE on the fracture surface.

in LBE at 300 °C was 175 kJ m^{-2} which is about 10% lower than the average J_Q value in air at 300 °C. A difference of 10% is within the normal scatter range found in fracture toughness tests, so the J_Q values showed no clear signs of LME.

The SEM pictures of the fracture surface are shown in Fig. 6C. The left picture shows an overview of the fracture surface created during the test. The flat areas on the left are a result of breaking the specimen after the test. The dark area with bright spots on the right of the fracture surface is some remainder of LBE which was not cleaned of by the cleaning solution. The detail of the fracture surface, shown in the right picture, shows no difference with the fracture surface in air. It is dimpled, indicating a ductile fracture mechanism. Apart from a relatively small difference in J_Q values for tests in both environments, there are no clear signs of LME of 316L steel.

4. Conclusion

Fracture toughness tests were performed using sub sized DCT specimens at 200 °C and 300 °C at displacement rate of 0.25 mm $(min)^{-1}$, in both air and oxygen saturated LBE environment. Two different steels were tested: ferritic–martensitic T91 steel and austenitic 316L stainless steel. The following conclusions can be made:

- Plane strain fracture toughness of T91 and 316L in LBE can be measured using normalisation methods due to the sufficiently high amount of ductility and toughness of these materials under the tested conditions.
- Plane strain fracture toughness of T91 is reduced in LBE. Based on these results, the maximum reduction of fracture toughness is 30% at 200 °C and 16% at 300 °C for tests at 0.25 mm $(min)^{-1}$.

- Fracture surface of T91 is clearly affected by the LBE which indicates that the embrittlement is most likely caused by LME.
- The plane strain fracture toughness of 316L is reduced in LBE within the normal scatter range without change in fracture surface appearance.

Acknowledgement

This work was partly supported by the European Project IP-EUROTRANS-DEMETRA (FI6W-CT-2004-516520).

References

[1] H. A Abderrahim, P. Kupschus, E. Malambu, Ph. Benoit, K. Van Tichelen, B. Arien, F. Vermeersch, P. D'Hondt, Y. Jongen, S. Ternier, D. Vandeplassche, Nucl. Instum. Meth. A 463 (2001) 487.
[2] W. Wagner, F. Groschel, K. Thomsen, H. Heyck, J. Nucl. Mater. 377 (2008) 12–16.
[3] T. Sasa, Prog. Nucl. Energ. 47 (2005) 314–326.
[4] J. Van den Bosch, D. Sapundjiev, A. Almazouzi, Nucl. Mater. 356 (2006) 237–246.
[5] W. Rostoker, J.M. McCoughy, M. Markus, Embrittlement by Liquid Metals, Reinhold, New York, Chapman and Hall, London, UK, 1960.
[6] Z. Hamouche-Hadjem, T. Auger, I. Guillot, D. Gorse, J. Nucl. Mater. 376 (3) (2008) 317–321.
[7] A. Legris, G. Nicaise, J.-B. Vogt, J. Foct, D. Gorse, D. Vançon, Scripta Mater. 43 (11) (2000) 997–1001.
[8] T. Sample, H. Kolbe, J. Nucl. Mater. 283–287 (2000) 1336–1340.
[9] J. Van den Bosch, ADS Candidate Materials Compatibility with Liquid Metal in a Neutron Irradiation Environment, Doctoral Thesis Ghent University, ISBN 978-90-8578-241-4, 2008.
[10] D. Kalkhov, M. Grosse, J. Nucl. Mater. 318 (2003) 143–150.
[11] B. Long, Y. Dai, J. Nucl. Mater. 376 (2008) 341–345.
[12] T. Auger, Z. Hamouche, L. Medina-Almazàn, D. Gorse, J. Nucl. Mater. 377 (2008) 253–260.
[13] J. Van den Bosch, G. Coen, A. Almazouzi, J. Degrieck, J. Nucl. Mater. 385 (2) (2009) 250–257.
[14] J.R. Donoso, J. Zahr, J.D. Landes, J. ASTM Int. 2 (3) (2005) 1–17.
[15] R. Chaouadi, J. Test. Eval. 32 (6) (2004) 469–475.
[16] T.L. Anderson, Fracture Mechanics: Fundamentals and Applications, third ed., CRC Press, Boca Raton, 2005.
[17] H. Ono, R. Kasada, A. Kimura, J. Nucl. Mater. 329–333 (2004) 1117–1121.
[18] A. Neimitz, I. Dzioba, J. Gałkiewicz, R. Molasy, Eng. Fract. Mech. 71 (2004) 1325–1355.